SANDIA REPORT

SAND201X-XXXX
Unlimited Release
Printed June 2017

Plenoptic Imaging for Three-Dimensional Particle Field Diagnostics

Daniel R. Guildenbecher, Elise M. Hall

Prepared by
Sandia National Laboratories
Albuquerque, New Mexico 87185 and Livermore, California 94550

Sandia National Laboratories is a multimission laboratory managed and operated by National Technology and Engineering Solutions of Sandia, LLC, a wholly owned subsidiary of Honeywell International, Inc., for the U.S. Department of Energy's National Nuclear Security Administration under contract DE-NA0003525.

Sandia National Laboratories

Issued by Sandia National Laboratories, operated for the United States Department of Energy by National Technology and Engineering Solutions of Sandia, LLC.

Printed in the United States of America. This report has been reproduced directly from the best available copy.

Available to DOE and DOE contractors from
U.S. Department of Energy
Office of Scientific and Technical Information
P.O. Box 62
Oak Ridge, TN 37831

Telephone: (865) 576-8401
Facsimile: (865) 576-5728
E-Mail: reports@osti.gov
Online ordering: http://www.osti.gov/scitech

Available to the public from
U.S. Department of Commerce
National Technical Information Service
5301 Shawnee Rd
Alexandria, VA 22312

Telephone: (800) 553-6847
Facsimile: (703) 605-6900
E-Mail: orders@ntis.gov
Online order: http://www.ntis.gov/search

SAND201X-XXXX
Printed June 2017
Unlimited Release

Plenoptic Imaging for Three-Dimensional Particle Field Diagnostics

Daniel R. Guildenbecher, Elise M. Hall
Diagnostics Science & Engineering
Sandia National Laboratories
P. O. Box 5800
Albuquerque, New Mexico 87185-MS0840

Abstract

Plenoptic imaging is a promising emerging technology for single-camera, 3D diagnostics of particle fields. In this work, recent developments towards quantitative measurements of particle size, positions, and velocities are discussed. First, the technique is proven viable with measurements of the particle field generated by the impact of a water drop on a thin film of water. Next, well controlled experiments are used to verify diagnostic uncertainty. Finally, an example is presented of 3D plenoptic imaging of a laboratory scale, explosively generated fragment field.

ACKNOWLEDGMENTS

The authors would like to thank Professor Brian Thurow at Auburn University for collaboration on the development of plenoptic imaging applications at Sandia as well as advising Elise M. Hall throughout the course of her graduate work. Numerous other students at Auburn also contributed to the initial development of these technologies, their contributions are gratefully acknowledged.

TABLE OF CONTENTS

1. Motivation 7
2. Introduction to Plenoptic Imaging 9
3. Development of Particle Tracking Methods 12
4. Quantifying Uncertainty 14
5. Application to Explosive Fragmentation 17
6. Next Steps 17
References 20

FIGURES

Figure 1. Example 3D particle fields requiring diagnostics of particle *size*, *position*, and *velocity*. (Left) a crown splash produced from the impact of a water drop on a thin water film [2]. (Right) Hypervelocity fragments produced from the detonation of a laboratory-scale explosive [3]. 7
Figure 2. Three-dimensional particle diagnostics using a three camera tomographic array [4]..... 8
Figure 3. Example 3D measurements using Digital Inline Holography (DIH). (Left) a crown splash produced from the impact of a water drop on a thin water film [2]. (Right) Hypervelocity fragments produced from the detonation of a laboratory-scale explosive [3]. 9
Figure 4. Raw plenoptic image of the crown splash produced from the impact of a water drop on a thin water film [ref]. Insert details the sub-images created by the microlens-array. [7] 10
Figure 5. Numerical refocusing of the instantaneous raw plenoptic image given in Fig. 4 [7].... 11
Figure 6. The plenoptic camera used for the results reported here [7]. 12
Figure 7. 3D plenoptic measurements of the crown splash produced from the impact of a water drop on a thin water film show in Figs. 4 and 5 [7]. 13
Figure 8. Numerically refocused plenoptic images of shotgun pellets [7]. 14
Figure 9. Numerically refocused plenoptic images of the stationary particle field used for uncertainty quantification [5]. 15
Figure 10. (a) Actual versus measured position for the particle circled in red in Fig. 9 and (b) a histogram of depth errors determined from many similar particle measurements [5]. 16
Figure 11. Numerically refocused plenoptic images of the hypervelocity fragment field from an RP-80 detonator.... 17

1. MOTIVATION

The dynamics of particle fields, which typically consist of disperse solid or liquid masses within a gaseous medium, are of broad scientific interest. The discussion herein focuses on those applications where a simultaneous understanding of particle *positions*, *sizes*, and *trajectories* are desired. For example investigations of liquid sprays for combustion applications typically require knowledge of the size and dispersion of liquid droplets in order to understand rates of mass transfer and combustion [1]. The left most image in Fig. 1 shows an experimental image of the crown splash created when a water droplet impacts a thin water film [2]. Quantification of the secondary droplet sizes and trajectories would inform modeling of mass transfer in this typical liquid spray process. In a distinctly different example, detonation of metal cased explosives generates fragments traveling at hypersonic velocities. The right most image in Fig 1 shows one example of a laboratory scale explosive [3]. Quantification of hazard zones produced by metal cased explosives requires knowledge of the fragment sizes, velocities, and trajectories. Applications range from the example shown in Fig. 1, which contains a few hundred mg of explosive, up to full-scale military munitions containing hundreds of kg of explosive.

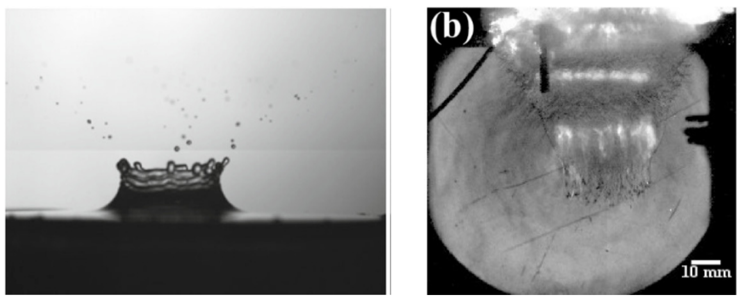

Figure 1. Example 3D particle fields requiring diagnostics of particle *size*, *position*, and *velocity*. (Left) a crown splash produced from the impact of a water drop on a thin water film [2]. (Right) Hypervelocity fragments produced from the detonation of a laboratory-scale explosive [3].

Although the two applications shown in Fig. 1 are distinctly different, the desired measured quantities and measurement challenges are similar. For these and many other related applications, a broad range of particle measurement techniques have been developed. In some cases, particles can be collected and analyzed after an experiment to quantify their size and morphology. During experiments, diagnostics include point measurement techniques such as laser Doppler velocimetry for velocity and phase Doppler anemometry for size. Other techniques are line-of-sight integrated, such as laser diffraction to quantify particle size distributions. Unfortunately, these types of diagnostics provide limited information on particle positions or trajectories. For that, two-dimensional (2D) imaging is widely used with Fig. 1 showing typical examples. With appropriately defined image processing routines it is possible to segment individual particle images and measure their 2D sizes and velocities. Temporal recording with digital cameras is straightforward, allowing these techniques to be further extended to resolve the time history of the particle sizes and positions within the 2D imaging plane.

Still, 2D imaging cannot quantify three-dimensional (3D) effects of particle shape or trajectories. One option to recover such information is to make use of multiple-tomographic cameras. For example, Fig. 2 shows select frames from high-speed imaging of fragments generated in a munition experiment [4]. Here, three separate cameras are used to image the fragments from three view angles. Camera calibration followed by triangulation allows for the recovery of the 3D fragment positions as shown in the upper right.

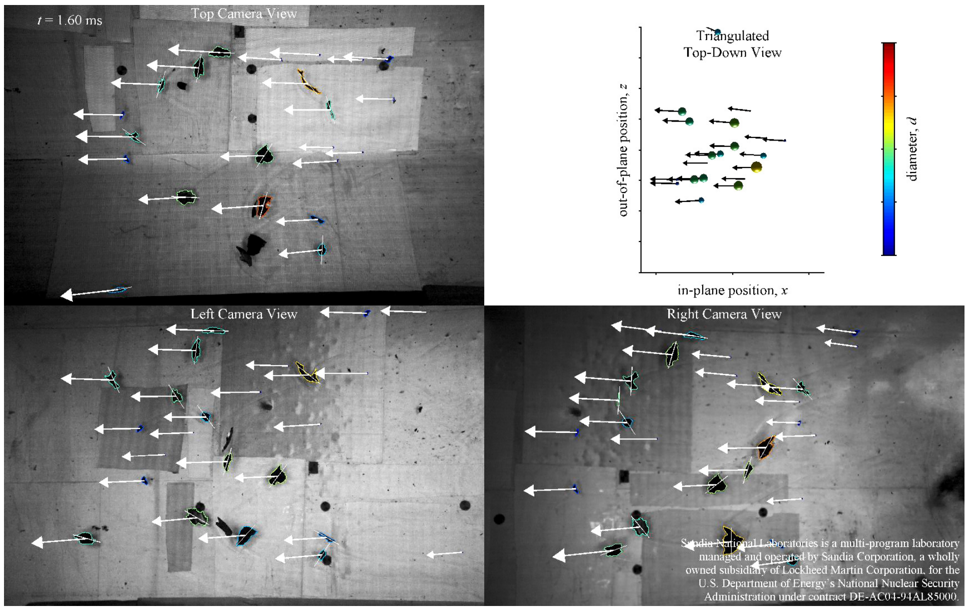

Figure 2. Three-dimensional particle diagnostics using a three camera tomographic array [4].

Unfortunately, multi-camera tomographic systems are expensive and require careful calibration. To increase the use of 3D particle measurement techniques, it is desired to reduce the overall cost and complexity of these experiments. Particularly for high-speed imaging applications, cameras are the single largest drivers of cost. Therefore, methods which reduce the total number of required cameras are particularly desired.

Previously the authors have explored digital in-line holography (DIH) for single-camera 3D measurements. This technique propagates a laser through the particle field and records the resulting diffraction patterns onto a digital sensor. With post processing it is possible to numerically refocus a single hologram and reconstruct 3D particle positions and velocities. For example, the left image in Fig. 3 shows the 3D crown-splash measured with DIH [2], while the right most image shows hypervelocity fragments from a lab-scale explosive also quantified with DIH [3]. As these examples illustrate, it is possible to capture 3D information of a particle field using DIH. However, a few challenges remain. For one, although DIH only requires a single camera, it does necessitate the use of a laser which increases experimental cost and complexity. Furthermore, the use of collimated and coherent light makes the images susceptible to beam steering through index-of-refraction gradients, resulting in schlieren and shadowgraph like effects. This is exemplified by the clear bow shocks around the hypervelocity fragments in Fig. 3. In this example, particles downstream of the initial fragment cannot be quantified due to the severe image distortion caused by these shock waves.

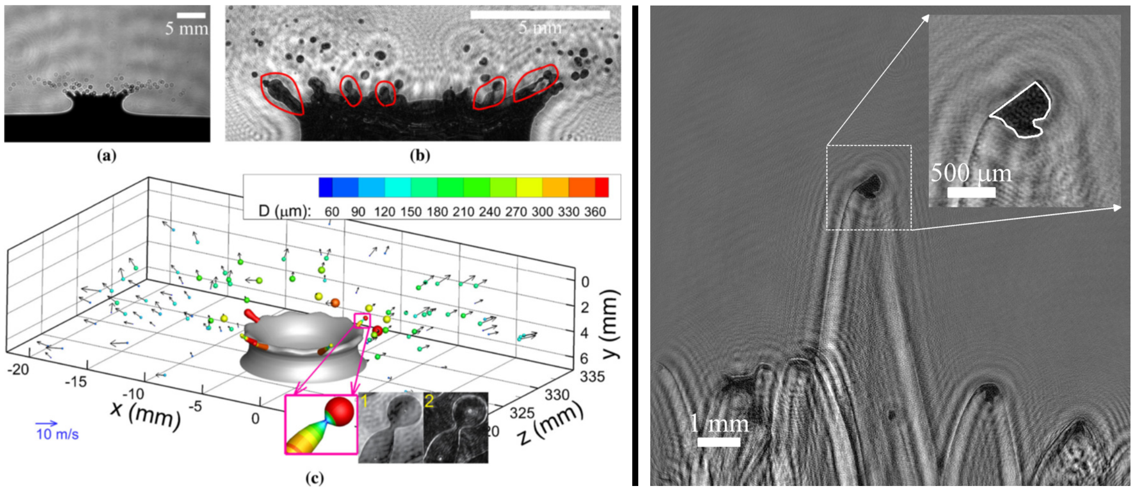

Figure 3. Example 3D measurements using Digital Inline Holography (DIH). (Left) a crown splash produced from the impact of a water drop on a thin water film [2]. (Right) Hypervelocity fragments produced from the detonation of a laboratory-scale explosive [3].

Here, an alternative measurement technique is discussed which is based on a plenoptic camera. This camera uses a microlens array to resolve spatial and angular information on incoming light rays in a manner that achieves single camera 3D imaging without lasers. The remainder of this work, summarizes the development of plenoptic imaging for 3D particle field measurements at Sandia National Laboratories from approximately 2015 to 2017. A number of the details of these developments have been published elsewhere [5-7] and the discussion here briefly summarize the important findings while referencing those works.

The main goals of the current report are to collect the lessons learned from the development of plenoptic imaging for 3D particle field measurements and provide guidance for future work, with particular focus on eventual applications to explosively generated fragments. The work begins with a brief explanation of plenoptic imaging. This is followed by a discussion of 3D particle tracking methods with initial application to the drop impact shown in the left hand image in Figs. 1 and 3. Following this, a more precise experiment is discussed which seeks to better quantify measurement uncertainty. Next, the first-ever application of plenoptic imaging to a laboratory-scale, explosively generated fragment field is presented. Finally, some potential next steps for this work are discussed.

2. INTRODUCTION TO PLENOPTIC IMAGING

A traditional camera integrates light rays entering at different angles through the lens aperature onto a single point, and therefore does not capture angular information. In contrast, a plenoptic camera, as investigated here, uses a microlens array between the main lens and image sensor to record sub-images of the light field within the aperture of the main lens. For example, Fig. 4 shows a raw plenoptic image of a similar water droplet splash to that shown in Fig. 1 [7]. The insert in the image details the individual sub-images created by the micro-lens array.

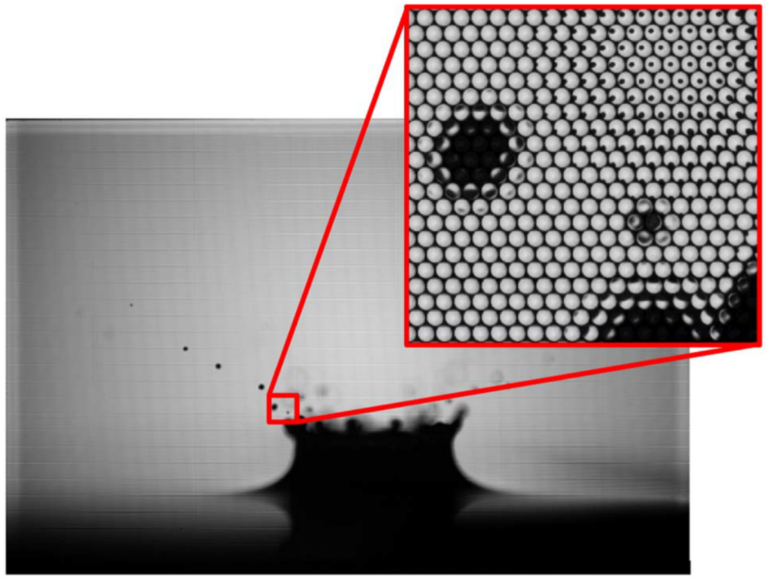

Figure 4. Raw plenoptic image of the crown splash produced from the impact of a water drop on a thin water film [ref]. Insert details the sub-images created by the microlens-array. [7]

With appropriate calibration, each pixel in the sensor plane is assigned a spatial position based on the center of the micro-lens and an angular position based on the location of the pixel within the sub-image. Once discretized in such a manner it is possible to use this information to perform numerical refocusing of the image as illustrated in Fig. 5 or create images at different perspectives within the range of angles captured by the main lens.

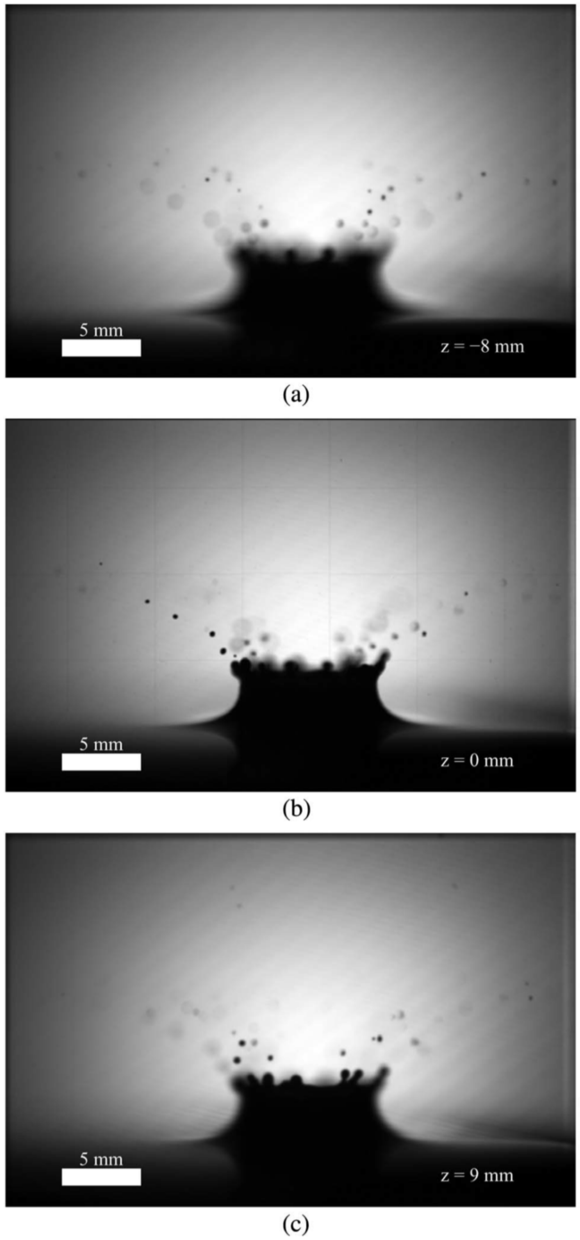

Figure 5. Numerical refocusing of the instantaneous raw plenoptic image given in Fig. 4 [7].

The plenoptic camera used in this work was constructed by the Advanced Flow Diagnostics Laboratory at Auburn University using an Imperx Bobcat B6620 29MP image sensor (6600 × 4400 pixels, pixel pitch, p_p = 5.5 µm). A microlens with 471 ×362 hexagonally arranged microlenses (microlens pitch, p_μ = 77 µm) is positioned with a custom mount at one micro lens focal length, f_μ = 308 µm, from the image sensor. Figure 6 shows the camera with a Nikon 105 mm front objective, which is the configuration used for the results reported here. The camera is compact and setup and alignment is similar to traditional photography. For these reasons, this technology holds particular promise for 3D measurements from a simple experimental configuration.

Figure 6. The plenoptic camera used for the results reported here [7].

Of course, this is not without its trandoffs. Importantly, achieving angular resolution generally requires that some spatial resolution is sacrificed. For example, in the current setup the spatial resolution is largely determined by the number of microlens. Therefore, the numerically refocused images, such as Fig. 5, have an effective spatial resolution of roughly 471 × 362 pixels, which is an order of magnitude less than the sensor size. While it is possible to construct different microlens and sensor combinations where this tradeoff is less severe and a so called 'Plenoptic 2.0' configuration has been proposed with different tradeoffs between spatial and angular resolution [8], overall the use of a plenoptic camera will require some sacrifice in terms of achievable spatial resolution. *Therefore for applications, it is important to determine if the advantages of 3D resolution outweigh the inherent reduction in 2D spatial resolution.*

The development of plenoptic imaging can be traced as far back as Lippmann in 1908 with the first description of light field imaging [9]. However, the concept was not feasible until the recent proliferation of digital sensors. The first implementation of a plenoptic camera was likely that of Adelson and Wang in 1992 [10]. More recently, Ng *et al* [11] proposed a compact, hand-held version of the plenoptic camera, which is the basis of the camera used here.

Following the developments of Ng *et al* [11], many researchers have explored plenoptic imaging for scientific measurements. Example applications include microscopy [12, 13], particle tracking for velocimetry measurements [14-19], spray imaging [20], etc.

3. DEVELOPMENT OF PARTICLE TRACKING METHODS

The first attempts at quantitative particle measurement using plenoptic imaging at Sandia explored the drop impact problem shown in Figs. 1, 4, and 5 [7]. This initial configuration was chosen because it was relatively easy to create in the lab, it had already been explored with DIH and therefore 3D data was available for comparison [2], and the flow displays symmetry which could be exploited to estimate measurement uncertainty. Here, the main findings are summarized, and significantly more details are available in Hall *et al* [7].

Figure 4 shows an example experimental image while Fig. 5 demonstrates the ability to refocus this image for resolution of out-of-plane particle positions. To achieve some temporal resolution, the plenoptic camera was operated in a double exposure configuration and backlit with a pulsed diode, similar to the methods commonly employed for double-exposure particle image velocimetry [21]. In this initial experiment, 3D particle localization and tracking was performed using methods originally developed for DIH [22-24]. Specifically, images were first numerically refocused to a large number of evenly spaced *z*-planes to create a three dimensional array of grayscale images. Next, the optical depths (*z*-positions) of individual particles were detected by searching for a maximum in image sharpness within sub-windows around each particles. Once located, particle sizes were measured from refocused images at these locations. Finally, a nearest neighbor matching routine was used to determine the particle displacements between the two frames recorded with 150 μs interframe time.

Fig. 7 shows an example of the resulting reconstructed top-down view of the droplet splash shown in Fig. 4 and 5. Results capture the expected flow symmetry of the droplet motion away from the center of impact. Further comparison of this result with previous DIH results in [2], confirm that the technique provides quantitative resolution of particle *position*, *size*, and *velocity* [7].

Inspection of the results in Fig. 7 appears to show some erroneous vectors in the out-of-plane, *z*-direction where a few individual measured velocities do not follow the overall flow symmetry. This is attributed to higher measurement uncertainty in the out-of-plane direction caused by the relatively narrow angular aperture from which this direction is reconstructed. This demonstrates a second important challenge in plenoptic imaging. While 3D resolution is achieved, angular information is only captured over the relatively narrow aperture of the front objective. *Therefore, measurements display significantly higher uncertainty in the depth direction, which complicates interpretation of results and may limit applications*. Of course, it should be noted that other single camera, 3D techniques, including DIH, suffer from similar tradeoffs [25].

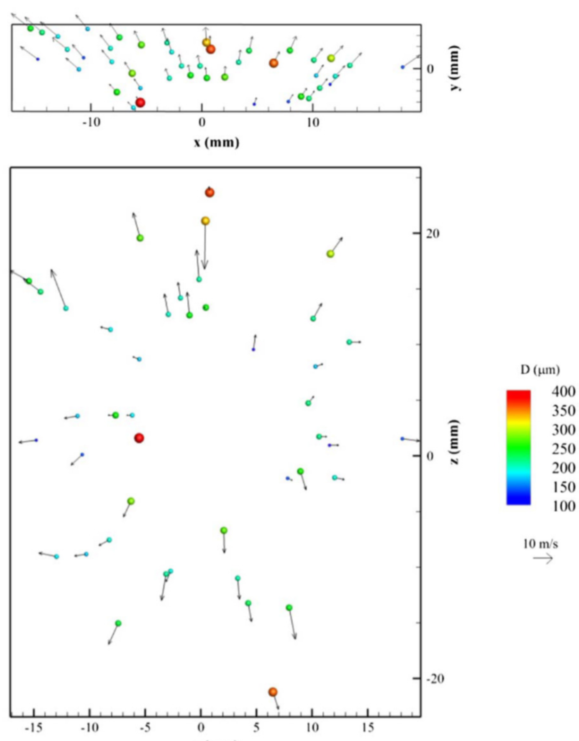

Figure 7. 3D plenoptic measurements of the crown splash produced from the impact of a water drop on a thin water film shown in Figs. 4 and 5 [7].

Finally, Hall *et al* [7] also considered plenoptic imaging of high-velocity particles. For example, Fig 8 shows 3D plenoptic imaging of pellets from a shot-gun, which are traveling near sonic velocities. No obvious image distortion caused by shockwaves can be seen in these images. In contrast, similar measurements were performed with DIH in Guildenbecher *et al*. [26]. In that work, the DIH results suffered from severe image distortion due to shock-waves. Because plenoptic imaging can capture 3D information from scenes illuminated with diffuse, white light it appears to have distinct advantages over DIH when investigating flows with significant index-of-refraction gradients.

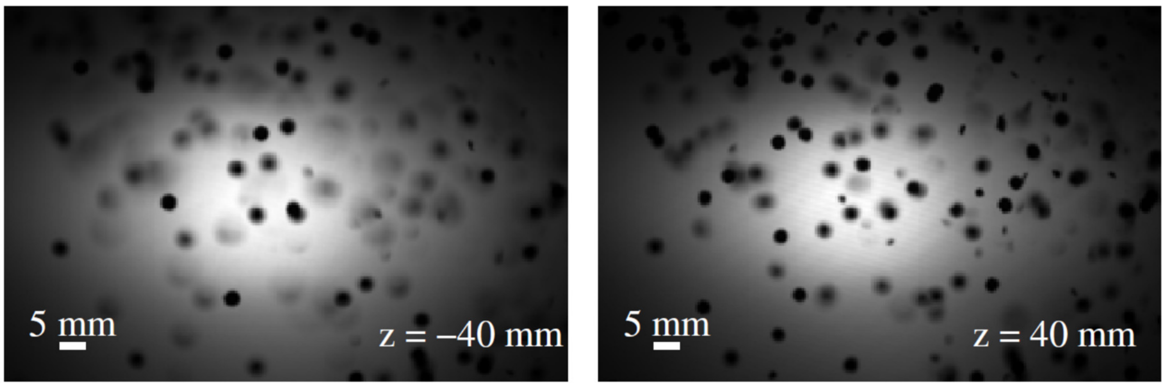

Figure 8. Numerically refocused plenoptic images of shotgun pellets [7].

4. QUANTIFYING UNCERTAINTY

It may be possible to optimize the data processing routines in order to minimize the depth uncertainty. Before doing so, it was decided to better quantify measurement uncertainty. For this, an experiment was conducted with the well-controlled particle field shown in Fig. 9. A fixed particle field was simulated using straight pins inserted into a rigid Styrofoam dome. This was placed onto an automatic traverse with good positional accuracy (specified absolute accuracy of ±4.5 μm.) aligned along the optical depth direction of the plenoptic camera. By translating the particle field through known distances and measuring those translations with the plenoptic camera, it is possible to quantify measurement uncertainty via comparisons to the exact values.

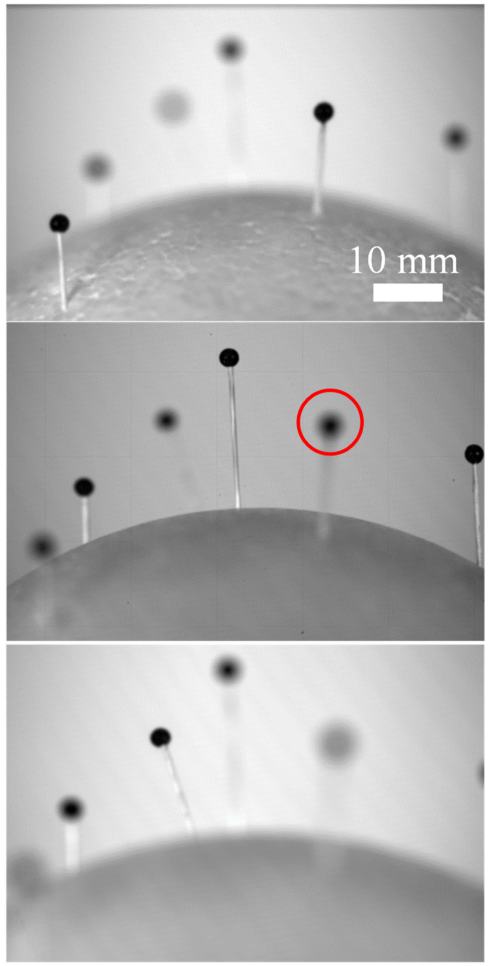

Figure 9. Numerically refocused plenoptic images of the stationary particle field used for uncertainty quantification [5].

Detailed investigation of these results is ongoing and is the planned topic of a future publication [5]. Some initial findings are given here. Figure 10(a) shows the measured position as a function of traverse position for the particle circled in red in Fig. 9. In general, good agreement is observed confirming overall accuracy of the diagnostic. Here, it is assumed that the differences between the measured positions and the best-fit line shown in Fig 10(a) is a quantitative measure of error. Figure 10(b) shows a histogram of all such error measurements for all particles measured over multiple realizations of the experiment shown in Fig. 9. Measurements can be performed using either a simple calibration based on thin lens equation to convert from image coordinates to physical coordinates or volumetric calibration to remove image aberration effects [6]. Figure 10(b) shows that the volumetric calibration clearly improves performance.

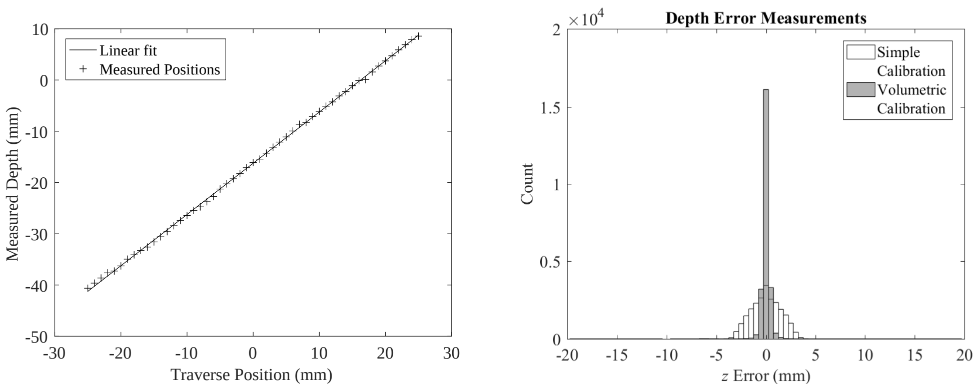

(a) (b)

Figure 10. (a) Actual versus measured position for the particle circled in red in Fig. 9 and (b) a histogram of depth errors determined from many similar particle measurements [5].

The theoretical depth resolution, Δz, of a numerically refocused image is derived Deem *et al*. [27],

$$\Delta z = f\left(M-1\right)^2\left[\frac{1}{M\left(M-1\right)-f_\mu N/f\left(N-2\right)}-\frac{1}{M\left(M-1\right)+f_\mu/f}\right] \tag{1}$$

where f is the focal length of the main lens, M is the nominal magnification, f_μ is the focal length of the microlenses, and N is the number of image sensor pixels behind each microlens (calculated as the microlens pitch, p_μ, divided by the pixel pitch, p_p). Initial analysis of the measurement precision, defined by the standard deviation of the error shown in Fig. 10(b), indicates that Eq. (1) provides a reasonable estimate of the actual measured depth errors, further details will be provided in [5].

In addition, the overall range of z-positions where accurate measurement can be performed is expected to fall within the depth-of-field, DOF, of images constructed from a single pixel behind each micro lens. Ng *et al*. [11] estimate this as

$$DOF = \left[\frac{Dl_o}{D-c}-l_o\right]-\left[\frac{Dl_o}{D+c}-l_o\right] \tag{2}$$

where $D = p_p \cdot l_i/f_u$, $c = -p_u/M$, l_o is the object distance, and l_i is the image distance. Initial analysis of the experimental error measurements Fig. 10 also appears to confirm that measurements are most accurate within the z-range defined by Eq. (2). Again, further details will be provided in [5].

Overall these results indicate that measurement error can be reasonably predicted by the optical properties of the plenoptic camera via Eqs. (1) and (2). Conversely, this also suggests that achievable measurement accuracy is largely fixed once the microlens and front objective is chosen. Currently, custom glass microlens arrays can be expensive. *Therefore, any new measurement application should carefully consider the tradeoffs in measurement accuracy and measurement volume given by Eq. (1) and (2), respectively, before designing and constructing custom plenoptic cameras.*

5. APPLICATION TO EXPLOSIVE FRAGMENTATION

The previous sections show that plenoptic imaging can be used for quantitative 3D particle measurements, is particularly advantageous in the presence of shockwaves when compared to DIH, and measurement uncertainty is reasonably well understood. Having achieved this, the final goal of the efforts discussed here was to demonstrate the ability to capture 3D images of explosively generated fragments. This was achieved by imaging the fragment field created by the detonation of an RP-80 detonator from Teledyne RSI. This detonator contains approximately 200 mg of explosive encased in a brass sleeve with an aluminum cup. Once detonated, the metal components fracture and are ejected at hypervelocities in a ring-like pattern. To image this, the detonator was placed within a Plexiglas boombox. The plenoptic camera shown in Fig. 6 was configured with approximately 0.4× magnification and positioned to view the detonator through a viewport. To freeze the motion of the hypervelocity particles, a high-intensity diode (CAVILUX Smart) was positioned to backlight the field-of-view through a second viewport, and configured to provide 500 ns pulsed emission synchronized with the camera exposure. To minimize image washout from the high intensity emission from the explosive, the camera was operated with the minimum 10 μs exposure and a bandpass filter was placed in front of the camera which passed the relatively narrow bandwidth of the diode. Finally, images were acquired at 52.75 μs after triggering of the fireset.

Figure 11 shows select numerically refocused images of the fragment field. These images clearly demonstrate the ability of plenoptic imaging to capture the 3D nature of this fragment field. It is also important to note that although these fragments are traveling at many thousands of meters per second into atmospheric air, no clear image degradation due to shock waves is observed. Quantitative 3D measurement of the fragment field, similar to Fig. 7, could be relatively easily achieved if these experiments were repeated at slightly longer imaging delays such that individual particles are well separated to ease automatic image segmentation.

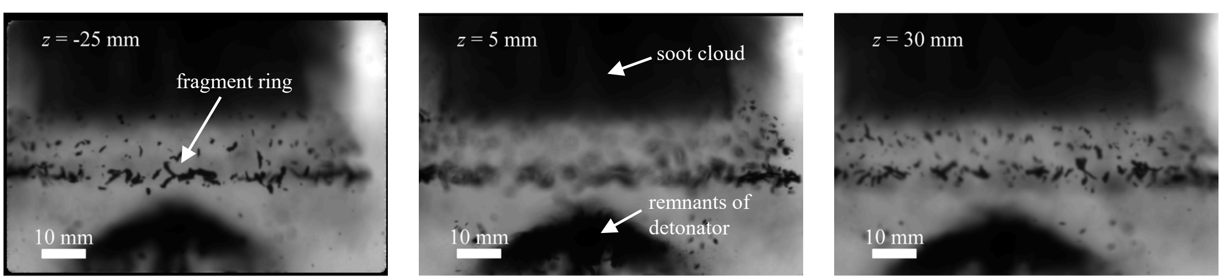

Figure 11. Numerically refocused plenoptic images of the hypervelocity fragment field from an RP-80 detonator.

6. NEXT STEPS

Here plenoptic imaging is demonstrated for single-camera, 3D quantification of particle fields. Particular focus is placed on application to diagnostics of explosively generated fragments. Specific advantages include the experimental simplicity and reduced susceptibility to image degradation due to index-of-refraction gradients. Challenges include inherent tradeoffs between 2D spatial resolution and depth resolution, higher measurement uncertainty in the depth direction, and the need for custom designed microlens-arrays.

Figure 11 specifically demonstrates this technology for diagnostics of explosively generated, hypervelocity fragments. For practical measurements, it will likely be necessary to combine this technology with high-speed cameras such that the 3D particle field can be temporally resolved. While high-speed digital camera technology has been rapidly progressing, such cameras still tend to have significantly fewer image sensor pixels compared to the large CCD array used here. Therefore, construction of a high-speed plenoptic camera will need to carefully consider the tradeoffs between spatial and angular resolution discussed here. For this, Eqs. (1) and (2) can serve as guides for the design of a custom microlens-array and front objective combinations that best balances the resolution demands of a specific application.

REFERENCES

1. Lefebvre, A.H., *Atomization and Sprays*. 1989, New York: Hemisphere Pub. Corp. xi, 421 p.
2. Guildenbecher, D.R., et al., *Digital in-line holography to quantify secondary droplets from the impact of a single drop on a thin film.* Experiments in Fluids, 2014. **55**: p. 1670.
3. Yeager, J.D., et al., *Characterization of Hypervelocity Metal Fragments for Explosive Initiation.* Journal of Applied Physics, 2017. **In-press**.
4. Sandia National Laboratories, *Technology Development for Understanding Uncertainties in Fragment Generation, Flight and Impact: FY16 Update*. 2017.
5. Hall, E.M., D.R. Guildenbecher, and B.S. Thurow, *Uncertainty Characterization of Particle Location Using a Plenoptic Camera.* In Preperation, 2017.
6. Hall, E.M., et al., *Volumetric calibration of a plenoptic camera.* In Preperation, 2017.
7. Hall, E.M., B.S. Thurow, and D.R. Guildenbecher, *Comparison of three-dimensional particle tracking and sizing using plenoptic imaging and digital in-line holography.* Applied Optics, 2016. **55**(23): p. 6410-6420.
8. Georgiev, T., G. Chunev, and A. Lumsdaine. *Superresolution with the focused plenoptic camera*. in *SPIE Computational Imaging IX*. 2011. January 23.
9. Lippmann, G., *La photographie integrale.* Comptes Rendus De L Academie Des Sciences, 1908. **146**: p. 446-551.
10. Adelson, E.H. and J.Y.A. Wang. *Signle lens stero with a plenoptic camera*. in *Pattern analysis and machine intelligence*. 1992.
11. Ng, R., et al., *Light field photography with a hand-held plenoptic camera*. 2005, Stanford University.
12. Pégard, N.C., et al., *Compressive light-field microscopy for 3D neural activity recording.* Optica, 2016. **3**(5): p. 517-524.
13. Kim, J., et al., *F-number matching method in light field microscopy using an elastic micro lens array.* Optics Letters, 2016. **41**(12): p. 2751-2754.
14. Timothy, W.F. and S.T. Brian, *3D Particle Position Reconstruction Accuracy in Plenoptic PIV*, in *52nd Aerospace Sciences Meeting*. 2014, American Institute of Aeronautics and Astronautics.
15. La Foy, R.R. and P. Vlachos. *Multi-camera plenoptic particle image velocimetry*. in *10th International Symposium on Particle Image Velocimetry*. 2013. Delft, The Netherlands.
16. Fahringer, T.W. and B.S. Thurow, *The Effect of Grid Resolution on the Accuracy of Tomographic Reconstruction Using a Plenoptic Camera*, in *51st AIAA Aerospace Sciences Meeting including the New Horizons Forum and Aerospace Exposition*. 2013, American Institute of Aeronautics and Astronautics.
17. Melnick, M., et al., *Experimental Investigation of Three-Dimensional Structures in an Adverse Pressure Gradient Turbulent Boundary Layer*, in *42nd AIAA Fluid Dynamics Conference and Exhibit*. 2012, American Institute of Aeronautics and Astronautics.
18. Lynch, K., T.W. Fahringer, and B. Thurow, *Three-Dimensional Particle Image Velocimetry Using a Plenoptic Camera*, in *50th AIAA Aerospace Sciences Meeting including the New Horizons Forum and Aerospace Exposition*. 2012, American Institute of Aeronautics and Astronautics.
19. Fahringer, T. and B. Thurow, *Tomographic Reconstruction of a 3-D Flow Field Using a Plenoptic Camera*, in *42nd AIAA Fluid Dynamics Conference and Exhibit*. 2012, American Institute of Aeronautics and Astronautics.

20. Nonn, T., V. Jaunet, and S. Hellman. *Spray droplet size and velocity measurement using light-field velocimetry*. in *ICLASS 2013, 12th Triennial International Conference on Liquid Atomization and Spray Systems*. 2013. Heidelberg.
21. Raffel, M., et al., *Particle Image Velocimetry: A Practical Guide*. 2^{nd} ed. 2007, Berlin: Springer.
22. Gao, J., et al., *Refinement of particle detection by the hybrid method in digital in-line holography.* Applied Optics, 2014. **53**(27): p. G130-G138.
23. Guildenbecher, D.R., et al., *Digital holography simulations and experiments to quantify the accuracy of 3D particle location and 2D sizing using a proposed hybrid method.* Applied Optics, 2013. **52**(16): p. 3790-3801.
24. Gao, J., et al., *Uncertainty characterization of particle depth measurement using digital in-line holography and the hybrid method.* Optics Express, 2013. **21**(22): p. 26432-26449.
25. Katz, J. and J. Sheng, *Applications of holography in fluid mechanics and particle dynamics.* Annual Review of Fluid Mechanics, 2010. **42**: p. 531-555.
26. Guildenbecher, D.R., et al., *Accurate measurement of out-of-plane particle displacement from the cross-correlation of sequential digital in-line holograms.* Optics Letters, 2013. **38**(20): p. 4015-4018.
27. Deem, E., A., et al., *On the resolution of plenoptic PIV.* Measurement Science and Technology, 2016. **27**(8): p. 084003.

DISTRIBUTION

1	Auburn University Department of Aerospace Engineering Attn: B. Thurow 211 Davis Hall Auburn University, AL 36849-5338		
2	MS0557	Nedra Bonal	Org. 1529
3	MS0828	Tracie L. Durbin	Org. 1512
4	MS0840	Stephen W. Attaway	Org. 1500
5	MS0899	Technical Library	9536 (electronic copy)

Sandia National Laboratories